Journal of Hazardous Materials 189 (2011) 54–61

Contents lists available at ScienceDirect

Journal of Hazardous Materials

journal homepage: www.elsevier.com/locate/jhazmat

Perchlorate removal by quaternary amine modified reed

Salem Baidas[a,c], Baoyu Gao[b], Xiaoguang Meng[a,*]

[a] Center for Environmental Systems, Stevens Institute of Technology, Hoboken, NJ 07030, USA
[b] School of Environmental Science and Engineering, Shandong University, Jinan 250100, PR China
[c] Environmental Sciences Department, Environment and Urban Development Division, Kuwait Institute for Scientific Research, P.O. Box 24885, Safat 13109, Kuwait

ARTICLE INFO

Article history:
Received 9 August 2010
Received in revised form 27 January 2011
Accepted 31 January 2011
Available online 4 February 2011

Keywords:
Perchlorate
Modified reed
Raman
Adsorption
Zeta potential

ABSTRACT

We report a kinetic and equilibrium study of perchlorate adsorption onto giant reed modified by quaternary amine (QA) functional groups in batch reactors. The effect of pH, contact time, and initial perchlorate concentration on removal was investigated. The adsorption capacity for perchlorate was 169 mg/g on the modified reed (MR) particles ranging in size from 100 to 250 μm. The isotherm results were best described by the combined Langmuir–Freundlich equation. Optimum removal occurred in the pH range 3.5–7.0 and was reduced at pH > 8.5. The maximum adsorption rate occurred within the first minute of contact and equilibrium was achieved within 7 min. A three-stage adsorption occurred. In stage 1, adsorption was rapid and was controlled by boundary layer diffusion. In stage 2, adsorption was gradual and was controlled by both boundary layer and intraparticle diffusion. In stage 3, adsorption reached a plateau. The kinetic results fit well with a pseudo second-order equation. The adsorption mechanism was explored using Zeta potential analysis and Raman spectroscopy. Zeta potential measurements showed that reed modification enhanced perchlorate removal by increasing the surface potential. Electrostatic attraction between perchlorate anion and positively charged quaternary amine groups on the MR was the primary mechanism responsible for perchlorate removal.

1. Introduction

Recently developed technologies have greatly aided environmental researchers in determining the scope of perchlorate contamination in the US [1]. Perchlorate (ClO_4^-) contamination has been reported in 26 states and Puerto Rico [2]. It has been detected in natural surface and ground waters that feed into US drinking water supplies [3–5]. This form of contamination is most common in the northeastern and southwestern coastal areas [6]. Perchlorate has also been detected in plants; food products, cow's milk, and human breast milk [7].

Increased interest in perchlorate detection and removal stems from the adverse health effects associated with its exposure [2]. Because perchlorate and iodide (I^-) have similar ionic charges and volumes – 3.94×10^{-23} cm^3 for ClO_4^- and 4.23×10^{-23} cm^3 for I^- [8] – perchlorate competes with iodide, inhibiting its uptake by the thyroid gland and reducing thyroid hormone production [1]. Thyroid hormones regulate several critical functions in the body, including oxygen consumption, metabolism, skeletal growth, and brain development [4]. Hypothyroidism has been associated with perchlorate exposure [6]. Perchlorate contamination poses a special danger to nursing mothers and infants, as perchlorate can be passed from mother to infant through breast milk, severely affecting development of thyroid function [9]. These children are more likely to develop permanent physical and mental disabilities, including mental retardation, Attention Deficit Hyperactivity Disorder (ADHD), impaired hearing, and language deficits [9]. The effects of perchlorate on development are not limited to humans; a recent study found that the sex ratio of larval–juvenile zebra fish treated with high levels of perchlorate (100–250 mg/l) is skewed towards females [10].

As of May 2010, the EPA had not set a standard for perchlorate in drinking water. However, in 2005 the National Resource Council recommended that the maximum daily intake of perchlorate not exceed 0.7 μg/kg [11], the equivalent of 25 μg/l for a 70 kg adult male with daily water consumption of 2 l. The state of California, on the other hand, has mandated 18 μg/l as the level at which remediation is required [12].

Perchlorate is widely used in the manufacture of commercial products such as road flares, air bags, and fireworks [13]. However, most perchlorate contamination is linked to military use [5]. Because of its rich oxygen content and highly oxidized form of chlorine, ammonium perchlorate salt (NH_4ClO_4) is widely used as an oxidant in rocket fuel [13–15].

There are natural sources of perchlorate contamination, such as the caliche deposits of the Atacama Desert in Chile. These deposits

* Corresponding author. Tel.: +1 201 216 8014; fax: +1 201 216 8303.
E-mail addresses: xmeng@stevens.edu, xmeng@stevens-tech.edu (X. Meng).

0304-3894/$ – see front matter © 2011 Elsevier B.V. All rights reserved.
doi:10.1016/j.jhazmat.2011.01.124

are rich in nitrate and perchlorate, which are often found together in nature [16]. Caliche deposits are used as a fertilizer in the United States, resulting in perchlorate contamination from surface water runoff or from leaching into groundwater [6]. Perchlorate, although thermodynamically unstable, is kinetically non-reactive at the low concentrations typically found in contaminated ground and surface water [17]. In addition, perchlorate salts have high solubility and low tendency to form complexes in water, making removal difficult.

Current treatment technologies such as ion exchange can effectively remove perchlorate and other ionic contaminants from ground and surface water [17–19]. However, a major problem of ion exchange is its cost. Regeneration of the spent resin produces brine that is concentrated in perchlorate and in salt (3–6% NaCl) which requires further treatment before final disposal [20,21]. Membrane filtration and reverse-osmosis technologies have proven to be even more expensive than ion exchange [22]. Biological reduction, in which bacteria use perchlorate as an electron acceptor, can be a useful and cost-effective alternative [20]. However, biodegradation is relatively slow and is extremely sensitive to pH and salinity changes. In addition, biological reduction requires further treatment to remove organic compounds and pathogens [23].

Plant-based adsorbents synthesized from agricultural waste have been successfully used to remove many anionic contaminants [24–26]. Agricultural waste is readily available and constitutes a waste stream itself if not utilized [27]. Giant reed (GR), *Arundo donax L.*, an agricultural waste product, is a fast-growing plant that is abundant in most countries around the world due to its easy adaptation to a variety of environments [28]. With high biomass potential (27–32 tons year^{-1} ha^{-1}), GR is readily available and inexpensive [29]. For example, GR stems are used as a wood alternative in the paper industry to produce high-quality chemical pulps [29]. GR was used as a precursor for activated carbon preparation by Vernersson et al. [30]. Reed is more resistant to biological degradation and should have longer life time in water treatment application than other agricultural materials, such as wheat and rice straw. The lifespan of reed used for thatching is usually between 40 and 60 years [31]. GR (whole stems, no leaves) is composed of lignin, cellulose, hemicellulose, and extractives such as fats, oils, and waxes [32,33]. Lignin, cellulose, and hemicellulose have many easily accessible hydroxyl groups that can be used for the attachment of various functional groups [32,33]. By attaching quaternary amines (QA) through chemical modification, GR can be transformed into an anion exchanger [34], termed modified reed (MR). MR can be used to remove anions, such as perchlorate, from water. Modified reed was successfully used in a pilot-scale filtration system to remove phosphate [35].

Although various functionalized adsorbents have been employed previously to remove perchlorate [24,36], adsorption of perchlorate using agricultural adsorbent modified with quaternary ammonium functional groups has not been reported. In view of the possibility that MR might provide an economical adsorbent useful for environmental perchlorate remediation [32–34], the current study was undertaken to investigate perchlorate adsorption on MR. Batch experiments were conducted to explore ClO_4^- and MR interactions at the interface. Adsorption isotherms were constructed and fitted to the experimental data. pH and concentration effects were studied to learn optimal adsorption conditions. As kinetic parameters are crucial to the design of treatment systems, we also conducted experiments to determine the uptake rate and the time needed to reach equilibrium. The data were fitted with a pseudo second-order model. Non-linear regression was used for isotherm and kinetic modeling.

Finally, to obtain deeper insight into the adsorption mechanism and the vibrational behavior of perchlorate in free and MR-sorbed states, we performed Zeta potential and Raman spectroscopy analysis. The spectroscopy data were correlated with adsorption data. This study therefore addresses the gap in the literature between quantitative studies of MR for adsorption and spectroscopic analyses of sorption mechanisms for perchlorate.

2. Materials and methods

2.1. Giant reed

The raw giant reed and the quaternized amine modified reed used in this study were provided by Dr. Baoyu Gao (School of Environmental Science and Engineering, Shandong University, China). GR (whole stems, no leaves) contains 21.1% lignin, 31.1% cellulose, 30.3% hemicellulose, and 12.1% extractives [32]. GR was reacted with epichlorohydrin, ethylenediamide, and triethylamine to form cellulose ether and then quaternary amine groups through cross-link [34]. MR is an anion exchanger, characterized by quaternary amine functional groups and particle size distribution of 100–250 μm. The total exchange capacity (TEC) of MR is associated with its nitrogen content which was determined to be 7.78%, while it was 0.9% in GR [34]. Based on the chemical composition of the quaternary amine group ($-CH_2CHOHCH_2NHCH_2CH_2NHCH_2OHCHCH_2N(CH_2CH_2)_3^+$, the content of the quaternary amine charge was about 1.64 eq(+)/g which is equal to an exchange capacity of 162 mg-ClO_4/g.

2.2. Reagents

All chemicals used were of ACS grade and obtained from Fisher Scientific. Tap water was aged for 24 h at room temperature before use and was used as the water source for all experiments. The average ionic strength of water determined by conductivity was 0.01 M. The water was supplemented with the required amounts of ClO_4^- from a stock solution containing 10,000 mg/l ClO_4^- prepared by dissolving 1.41 g sodium perchlorate monohydrate ($NaClO_4{\cdot}H_2O$) in 100 ml of deionized water (DI) (18.2 MΩ cm, Millipore, Cambridge, MA). Working standards were prepared daily from the stock solution.

2.3. Adsorption studies

Kinetic studies were carried out using 0.1 g MR in 50 ml suspension containing 10, 20, and 30 mg/l ClO_4^- or 0.1 g GR in a 50 ml suspension containing 10 mg/l (ClO_4^-). Mixing was carried out at room temperature (25 °C) in 125 ml bottles with a magnetic stirring bar on a magnetic stirrer. Samples were drawn at 0, 1, 3, 5, 7, 10, 14, 15, 20, 25, 30 min, and 24 h, the last sampling time being sufficient to reach a steady state. The pH was maintained at 7.0 ± 0.5 with addition of 0.1 M HCl and NaOH. Samples were collected in 1.5 ml Micro centrifuge® tubes, then placed in a Micromax® centrifuge at a mixing speed of 10,000 RPM for 10 min. After centrifuging, 1.0 ml of the supernatant was withdrawn and placed in 2.0 ml clear glass vials for perchlorate analysis using ion chromatography. The amount of adsorbed perchlorate q_t (mg/g) at any time was calculated as follows:

$$q_t = \frac{(C_i - C_t)V}{m} \quad (1)$$

where C_i is the initial concentrations (mg/l) of perchlorate, C_t is the concentrations (mg/l) of perchlorate at any time, V is the volume of solution (ml), and m is the dry mass of the adsorbent (g).

Isotherm tests were performed to determine MR adsorption capacity for (ClO_4^-). MR (0.1 g) was added to 50 ml tap water containing 3, 10, 30, 50, 100, 150, 300, 500, 700, or 900 mg/l (ClO_4^-). Mixing was performed in 125 ml bottles placed on a rotary mixer at 150 RPM (Glas-Col, 2128, Terre Haute, IN) for 24 h to reach equilibrium at room temperature (25 °C). The pH of each sample was

maintained at 7.0 ± 0.5 with 0.1 M HCl and NaOH. Perchlorate was analyzed in supernatants collected from samples.

The ion chromatograph (Dionex IC25) used for perchlorate analysis included an analytical pump, an Eluent Generator (EG40), a Conductivity Detector (CD25), an Auto Sampler (AS50), a column enclosure (LC20), an Ion-Pac® AS16 (4 mm × 250 mm) column, a sample injection loop with a capacity of 1000 μl, and a current suppressor (ASRS Ultra II). Chromeleon® version 6.4 software was used for instrument control and data collection. All components of the instrument, including the software, were made by Dionex Corporation (Sunnyvale, CA). An EluGen® potassium hydroxide cartridge was used as the eluent at 50 mM KOH concentration and a pump flow rate of 1.0 ml/min. Current suppression was set at 100 mA. The sample injection volume was 250 μl, and the running time was 18 min. With this setup, the detection limit was 0.1 mg/l.

2.4. pH and Zeta potential effects

To determine the effect of pH on perchlorate removal, additional samples of 0.1 g MR in 50 ml tap water containing 30 mg/l ClO_4^- or 0.1 g GR in 50 ml tap water without ClO_4^- were prepared in which the pH varied from 3.5 to 10.5. Samples were mixed in 125 ml bottles placed on a rotary mixer at 150 RPM for 24 h at room temperature (25 °C). After mixing, the samples were analyzed for aqueous perchlorate and for equilibrium pH. In addition, Zeta potential was measured for GR samples. Aliquots of the equilibrated suspensions were withdrawn into clear disposable Zeta cells using Luer-lok syringe and injected into a Malvern Zetasizer. Each sample was run in triplicate.

Zeta potential was measured using a Zetasizer Nano series® instrument (Malvern Instruments, Worcestershire, UK). The parameters were set for dilute water samples: a temperature of 25 °C, a dielectric constant of 78.5, a viscosity of 0.88 cP, and an applied voltage of 150 mV. The Zeta potential was determined by measuring the electrophoretic mobility (U_E), which is related to the Zeta potential (ζ) by Henry's equation [37]:

$$U_E = \frac{2\varepsilon\zeta f(Ka)}{3\eta} \quad (2)$$

where ε is the dielectric constant, η is the viscosity, and $f(Ka)$ is Henry's function. The Smoluchowski approximation was used, which assigns a value of 1.5 to $f(Ka)$, suitable for moderate electrolyte concentrations in aqueous media. Dispersion tech® version 5.0, a Malvern software, was used for instrument control and data collection.

2.5. Raman spectroscopy

Raman spectroscopy was used to explore ClO_4^- vibrational behavior in the free and MR-sorbed states. To increase the signal-to-noise ratio, a highly concentrated perchlorate solution was used for the Raman analysis. MR (0.1 g) was added to 50 ml of DI water containing 10,000 mg/l ClO_4^- and mixed for 24 h at 150 RPM on a rotary mixer. Equilibrium pH values ranging from 2.0 to 10.5 were maintained with 0.1 M HCl and NaOH. Microscope slides were soaked in Piranha solution (3:1 concentrated H_2SO_4 to 30% H_2O_2) for 40 min, rinsed thoroughly with DI water, then dried with oxygen-free nitrogen gas (AGL Welding, Clifton, NJ). Samples were placed evenly on glass microscope slides and analyzed while wet. Reference spectra were obtained for a 10,000 mg/l ClO_4^- solution without MR and for solid sodium perchlorate monohydrate $NaClO_4 \cdot H_2O$.

Raman spectra were collected using a Nicolet Almega™ dispersive Raman spectrometer equipped with a 780 nm laser. Spectra were collected between 1100 and 750 cm^{-1}, with a resolution of 4 cm^{-1}. The exposure time was 2 s. Thermo Scientific OMNIC™ Specta™ software was used for instrument control and data collection.

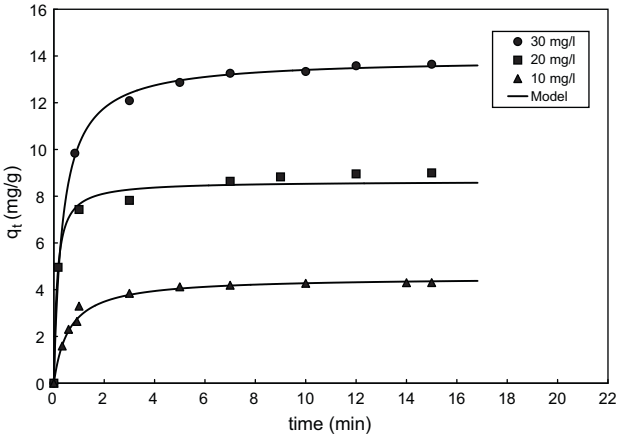

Fig. 1. Adsorption kinetics and the fitted pseudo-second-order model of perchlorate adsorption by MR. pH 7.0 ± 0.5; adsorbent dose: 2.0 g/l.

3. Results and discussion

3.1. Kinetic studies

Kinetics experiments were conducted to determine the uptake rate and equilibrium time. As shown in Fig. 1, for all perchlorate concentrations, the amount of perchlorate adsorbed q_t at time t increased with time and with initial perchlorate concentration eventually reaching an equilibrium q_e within 7 min. Rapid perchlorate adsorption onto activated carbon and exchange resin was also reported [23]. Before reaching the equilibrium stage, two distinct adsorption stages were observed. Stage 1, signified by a steep slope, reflected the rapid adsorption rate during the first minute of contact time during which most perchlorate removal occurred (80–85%). Stage 1 was extremely rapid and could be attributed to instantaneous monolayer adsorption of perchlorate at the MR surface [38]. Stage 2 (1 min < t < 7 min) represented by a gentle slope, was characterized by a gradually decreasing adsorption rate prior to reaching equilibrium (stage 3, t > 7 min). The reduced adsorption rate in stage 2 could reflect rearrangement of perchlorate adsorbed on the surface and a more thorough utilization of adsorption sites in the MR [23]. Similar kinetic stages of nitrate adsorption, by modified wheat residue on quaternary amine anion exchanger, have been reported [38]. In the first stage, the sorbate molecules are sorbed on the surface in the absence of other sorbate molecules, minimizing sorbate–sorbate interactions, leading to the formation of a monolayer. As this monolayer approaches saturation, a process of rearrangement may occur (stage 2), which involves further increases in sorbate molecules. At stage 3, the system has reached equilibrium.

3.2. Kinetics models

The kinetic data were fitted to a pseudo second-order kinetic equation [39]. Due to the inherent bias that results from linearization, a nonlinear function was used to fit the experimental data by minimizing the sum of squared residuals (*SSE*) [40]. The Solver tool in Microsoft Excel software was used to perform these calculations. The following form describes many heterogeneous adsorption reactions well [36]:

$$q_t = \frac{q_e k_2 t}{1 + q_e k_2 t} \quad (3)$$

Table 1
Kinetic parameters for adsorption of ClO_4^- by 2 g/l MR at pH 7.0 ± 0.5.

Pseudo second-order					Intraparticle diffusion		
C_i (mg/l)	K_2 (g/mg min)	q_e (mg/g)	R^2	SSE	K_p (mg/g min$^{0.5}$)	Z	R^2
10	0.41	4.51	0.99	0.20	0.67	2.64	0.99
20	0.81	8.80	0.99	0.63	0.74	6.64	0.98
30	0.20	13.88	0.99	0.17	2.01	8.24	0.96

In Eq. (3), q_e is the sorbed concentration at equilibrium (mg/g), q_t is the sorbed concentration at any time (mg/g), and K_2 is the pseudo second-order constant (g mg^{-1} min^{-1}). The values of the coefficients of determination were all high ($R^2 > 0.99$) and the sum of squared residuals were low (Table 1), indicating that pseudo second-order model calculation parameters (Eq. (3)) and the experimental data are in good agreement. In contrast, the pseudo first-order model provided a poor fit to the data (not shown). As also shown in Table 1, the rate constant k_2 (g mg^{-1} min^{-1}) increased from 0.41 to 0.81 as the perchlorate concentration increased from 10 to 20 mg/l. However, as the perchlorate concentration further increased to 30 mg/l, k_2 decreased to 0.20 (g mg^{-1} min^{-1}). The initial increase in perchlorate concentration resulted in a higher driving force that reduced the film layer thickness between the adsorbate and the adsorbent surface [41]. However, with the further increase in initial perchlorate concentration, the number of vacant and easily accessible adsorption sites is reduced. As a result, the time for adsorption to reach equilibrium is extended and the rate constant k_2 (g mg^{-1} min^{-1}) is reduced [42,43].

Understanding the adsorption mechanism is important in designing the most suitable treatment system. As the pseudo second-order kinetic model cannot identify the diffusion mechanism, kinetic results were further analyzed using an intraparticle diffusion model (IPD) to test for the contribution of intraparticle diffusion of the adsorbed perchlorate anions from the surface to available adsorption sites inside the pores. The transport of an adsorbate is governed by either boundary-layer diffusion or intraparticle diffusion or by both [44]. The IPD rate varies with the square root of time, as given by the Weber–Morris equation [45]:

$$q_t = k_p t^{0.5} + Z \quad (4)$$

In Eq. (4), k_p is the intraparticle diffusion rate constant (g mg^{-1} min$^{-0.5}$), Z is a constant relating to the thickness of the boundary layer, and t is the mixing time (min). According to the model, if the plot of q_t as a function of $t^{0.5}$ is linear, and passes through the origin, IPD is the only rate limiting step [46]. On the other hand, if the IPD plot exhibits multi-linearity, then boundary diffusion also plays a role, its contribution determined by the magnitude of the intercept Z [47].

Using the experimental data shown in Fig. 1, the linearized plot of the IPD model was fitted to the experimental data. The intraparticle diffusion constant, k_p from Eq. (4) was determined from the slopes of the lines in Fig. 2, while the intercept Z relating to the boundary layer diffusion. Model data parameters are summarized in Table 1. The IPD plot (Fig. 2), exhibits multilinearity suggesting that both boundary layer and IPD are involved in perchlorate uptake by MR. For the perchlorate concentrations of 10, 20, and 30 mg/l (ClO_4^-), k_p was 0.67, 0.74, and 2.01 (mg/g min$^{0.5}$), and Z was 2.64, 6.64, and 8.24, respectively. Both IPD and boundary layer effects increased with increasing perchlorate concentration (indicated by increasing k_p and Z values). Other studies have reported similar findings [48].

The results (Fig. 1 and Fig. 2) indicated that adsorption rate was controlled by boundary layer diffusion at the initial adsorption stage ($t < 1$ min), and was responsible for 80–85% of total removal. Both intraparticle and boundary layer diffusion controlled the adsorption rate during stage 2 ($1 < t < 7$ min), which was responsible for 10–15% of total removal.

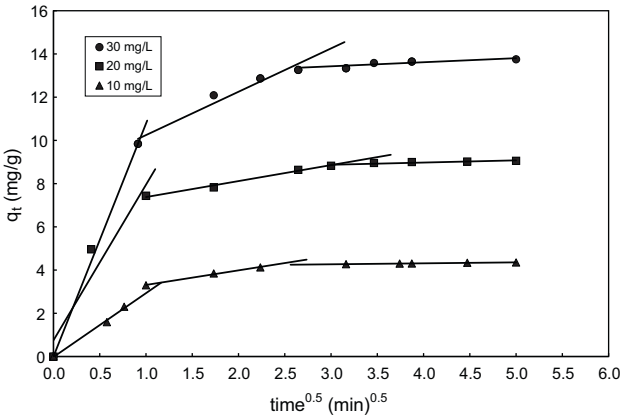

Fig. 2. Intraparticle diffusion model of perchlorate adsorption by MR. pH 7.0 ± 0.5; adsorbent dose: 2.0 g/l.

3.3. Isotherm studies

Isotherm studies were carried out as described in Materials and Methods (Section 2.3). Equilibrium results (Fig. 3) were tested for fit with the Langmuir, Freundlich, and Freundlich–Langmuir models. The Langmuir model assumes monolayer adsorption with maximum adsorption upon monolayer saturation, no interaction between the adsorbed anions species, and constant adsorption energy on all sites. The Langmuir model [49] is described by Eq. (5):

$$q_e = \frac{q_{max} K_L C_e}{1 + K_L C_e} \quad (5)$$

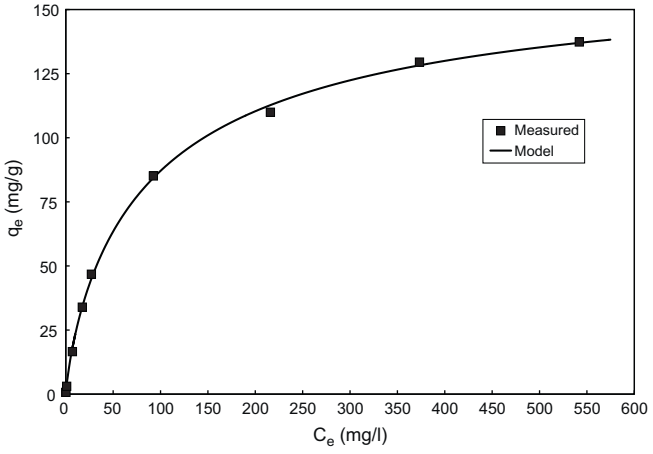

Fig. 3. Adsorption equilibrium results and the fitted Langmuir–Freundlich isotherm model of perchlorate adsorption by MR. Adsorbent dose: 2.0 g/l; pH 7 ± 0.5; contact time: 24 h.

In Eq. (5), q_e is the amount of perchlorate adsorbed (mg/g), C_e is the equilibrium concentration (mg/l), q_{max} is the maximum adsorption capacity (mg/g), and K_L is the Langmuir coefficient relating to adsorption intensity (l/mg). K_L is independent of the degree of adsorption (surface coverage) because uniform adsorption energy is assumed among adsorption sites on the homogenous surface [50,51]. The Freundlich model, unlike the Langmuir model, assumes that the adsorbent surface is heterogeneous with multiple adsorption layers [52]. Therefore, adsorption energy varies among adsorption sites. However, the maximum adsorption capacity is not defined in the Freundlich model [53]. The Freundlich model [54] is described by Eq. (6):

$$q_e = K_f C_e^n \quad (6)$$

where k_f is the Freundlich constant relating to the strength of adsorbate–sorbent interactions [(mg/g)/(mg/l)], and n is a dimensionless exponent between 0 and 1 relating to the degree of surface heterogeneity. For $n = 1$, Eq. (6) reduces to the classic linear equation. The modified Freundlich–Langmuir model [55] combines elements of both models by adding the exponent a, to account for surface heterogeneity. For a homogeneous surface $a = 1$, and Eq. (7) reduces to the Langmuir equation:

$$q_e = \frac{q_{max}(K_{LF}C_e)^a}{1 + (K_{LF}C_e)^a} \quad (7)$$

Parameters of the three isotherms are summarized in Table 2. The Langmuir–Freundlich isotherm provided the best fit (Fig. 3) as it had the lowest residuals ($SSE = 16.35$). The better fit of this model might be explained by the addition of the exponent (a) in (Eq. (7)) to account for heterogeneity of the MR surface. Best fit values for MR were: $q_{max} = 169.34$ (mg/g), $K_{LF} = 0.01$ (l/mg), and $a = 0.82$. As predicted by the model, the amount of perchlorate adsorbed at equilibrium increased with the increase in initial perchlorate concentration. The adsorption capacity of MR for perchlorate is much higher than that of activated carbon and lower than perchlorate-selective strong-base exchange resin [23].

The effect of the isotherm shape on the favorability of adsorption can be expressed by R_L, a dimensionless constant separation factor given in Eq. (8) [56]:

$$R_L = \frac{1}{1 + K_{LF}C_i} \quad (8)$$

$R_L > 1$ for unfavorable adsorption, $R_L = 1$ for linear adsorption, $0 < R_L < 1$ for favorable adsorption, and $R_L = 0$ for irreversible adsorption. The best-fit Langmuir–Freundlich parameters yielded $R_L < 1$, indicating favorable adsorption.

3.4. pH and Zeta potential effects

Fig. 4 shows the effect of pH on ClO_4^- adsorption by MR. Maximum removal obtained was 90% in the pH range 3.5–7.0. Adsorption decreased by 10% as the pH was increased to 7.8. Adsorption decreased by 40% as the pH was increased from 8.0 to 10.7. This accelerating decrease could be explained by competition between hydroxide anions and perchlorate anions at high pH values. In addition, decreased surface charge at high pH would be expected to weaken the electrostatic attraction between the perchlorate anions and the MR surface. Interestingly, more than 50% removal was observed at pH > 10.5 (Fig. 4), which could be attributed to the known pH independence of the charge status of quaternary amine functional groups [23].

The effect of reed modification (functionalization) with the quaternary amine functional group and pH on the surface charge was studied by comparing the Zeta potential of clean GR and cleans MR as a function of pH (Fig. 5). Over the entire pH range studied (3–11), the Zeta potential of GR was negative and was lower than

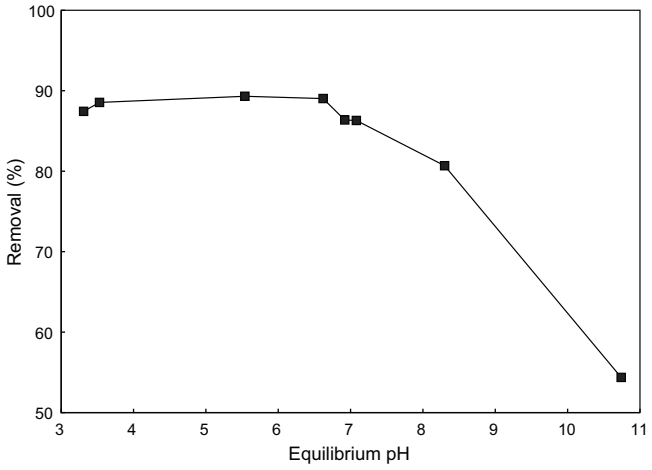

Fig. 4. Effect of pH on perchlorate adsorption by MR. Initial ClO_4^-: 30 mg/l; adsorbent dose: 2.0 g/l; contact time: 24 h.

the Zeta potential of MR. The Zeta potential of clean GR decreased from −1.43 to −20.2 mV as the pH increased from 3.5 to 10.7, whereas the Zeta potential of clean MR decreased from +27.1 to −1.7 mV as the pH increased from 3.4 to 11.4 (all values ± 0.3). Thus, the incorporation of QA functional groups into GR increased the surface potential of reed. These findings are in agreement with published data [23,25,32,37]. The fact that perchlorate removal was not obtained with GR while 85–90% removal was obtained with MR suggests that the QA functional group is largely responsible for the ability of MR to remove perchlorate from solution. Because Zeta potential is more negative at higher pH values, adsorption of perchlorate anions is expected to be reduced due to electrostatic effects. Our data show a positive correlation between perchlorate removal and Zeta potential (compare Fig. 4 and Fig. 5).

As pH increases, the electrostatic attraction between the MR surface and added anions will decrease along with the Zeta potential until the Zeta potential approaches the point of zero charge (PZC) for clean MR which was high at 11.3 (pH units), indicating preferential adsorption of OH^- over H^+ as expected from the positively charged functional groups on MR surface [57,58].

The effect of perchlorate adsorption on the Zeta potential of clean MR was studied. When ClO_4^- was added to clean MR, the Zeta potential decreased (Fig. 5). The decrease was the result of neutralization of the positive functional groups by the adsorbed perchlorate. An insignificant shift (less than 0.7 pH units) was

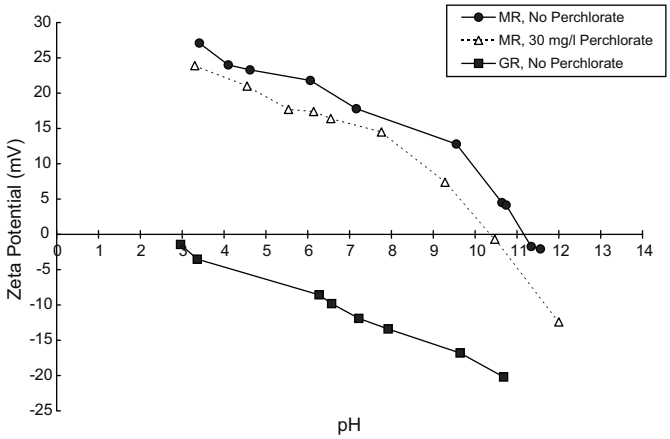

Fig. 5. Zeta potential for raw giant reed (GR) and modified reed (MR) shows the effect of modification and ClO_4^- addition on reed's surface charge. Adsorbent dose: 2.0 g/l; contact time: 24 h.

Table 2
Isotherm parameters for adsorption of ClO_4^- by 2 g/l MR at pH 7.0 ± 0.5.

Langmuir				Freundlich				Langmuir–Freundlich				
K_L (l/mg)	q_{max} (mg/g)	R^2	SSE	K_f (mg/g)/(mg/l)	n	R^2	SSE	K_{LF} (l/mg)	q_{max} (mg/g)	a	R^2	SSE
0.01	150.22	0.99	68.71	12.16	0.39	0.97	537.84	0.01	169.34	0.82	0.99	16.34

observed in the PZC value when 30 mg/l ClO_4^- was added to clean MR suggesting that interactions between MR and ClO_4^- are largely electrostatic attraction.

3.5. Raman measurements

Raman analysis was used to examine perchlorate–MR interaction by probing for shifts in the stretching bands when aqueous perchlorate was adsorbed onto MR. The symmetric stretching vibration band (ν_1) of the anion is commonly measured because its position varies with ion association and ion–ion interactions [59]. Stretching bands are well-defined in the Raman spectra. We recorded reference spectra of the (ν_1) mode for perchlorate in many phases to study the effects of perchlorate ion–ion association on the vibrational spectrum. As the Raman instrument resolution was 4 cm^{-1}, shifts of ~4 cm^{-1} were attributed to experimental error.

As shown in Fig. 6, a Raman peak for ClO_4^- in 0.1 M $NaClO_4$ was detected at 933 cm^{-1}. It is attributed to the strong Cl–O bonds of the tetrahedral perchlorate anion [60]. The 933 cm^{-1} band corresponds to free perchlorate ions in aqueous solution, as established in several independent studies [61,62]. The perchlorate band in solid $NaClO_4$ salt occurred at 953 cm^{-1}, a figure also reported in several studies [63–65]. Yoon et al. [23] reported a ClO_4^- peak at 951 cm^{-1} in $NaClO_4$ salt, and suggested that the peak corresponded to ($Na^+ \cdots ClO_4^- \cdots Na^+$) trimers, tetramers, or higher-order structures in the solid phase. Raman spectra of MR samples loaded with ClO_4^- gave a peak at 932 cm^{-1}. The same band position of the soluble and adsorbed perchlorate showed no specific interaction between the adsorbed perchlorate and MR. Yoon et al. [23] reported perchlorate peak detection on a strong base anionic resin (SR-7) at 930 cm^{-1}. Furthermore, Brooksby and Fawcett [66] found that ammonium functional groups had no effect on perchlorate ion association.

The effects of pH on the Raman spectra were studied for perchlorate–MR samples (Fig. 7). Peak positions for adsorbed perchlorate at pH 2.0, 6.6, and 10.5 had a negligible frequency shift of ~1–2 cm^{-1}, indicating that perchlorate ion association in the perchlorate–MR system was pH-independent. However, peak intensity varied with pH depending on the amount of perchlorate adsorbed, as previously established in Fig. 4. Peak intensity quantification was not studied in this paper.

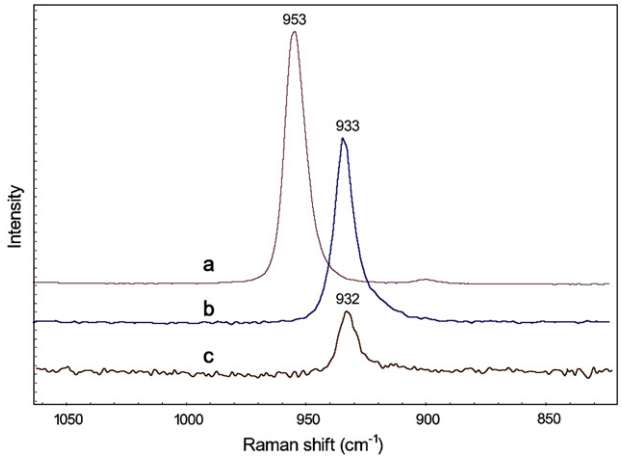

Fig. 6. Raman spectra of (a) reagent $NaClO_4$ salt; (b) 10^4 mg/l ClO_4^- solution; and (c) MR equilibrated with 10^4 mg/l ClO_4^- solution. Adsorbent dose: 2.0 g/l; pH 7.0 ± 0.5; contact time: 24 h.

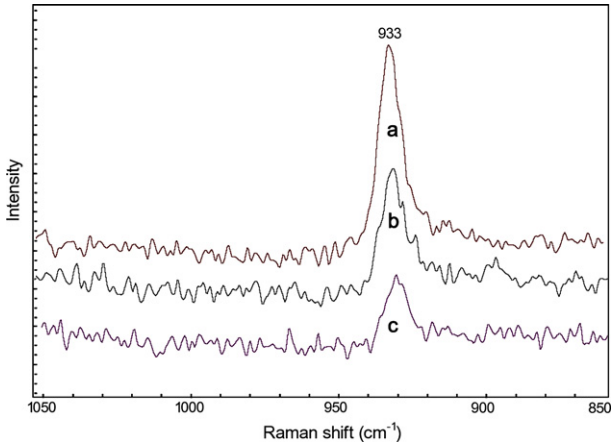

Fig. 7. Raman spectra (baseline-corrected) of adsorbed ClO_4^- on MR, which had been equilibrated for 24 h with 10^4 mg/l ClO_4^- solution at various pH values: (a) pH 6.6; (b) pH 2.0; and (c) pH 10.5. ClO_4^- loaded MR samples were prepared from $NaClO_4$ salt.

4. Treatment of perchlorate on spent MR

Treatment of perchlorate on spent MR is a critical issue for safe disposal of the used bio-sorbent or for reuse. A perchlorate-loaded spent MR was prepared by mixing 0.10 g MR with 50 ml of aged tap water containing 30 mg/l of ClO_4^-. A biological process was used for the destruction of the perchlorate by mixing the spent MR with perchlorate-reducing mixed bacteria in a closed container. The mixed bacteria were cultivated and enriched using anaerobic sludge collected from the wastewater treatment plant in Bergen County, NJ following the procedures described by Wang et al. [67]. Total digestion analysis determined that perchlorate content in the spent MR was 14 mg/g. After 4 and 7 days of biological reaction, the total perchlorate content on the MR was reduced to 1.4 and 0.25 mg/g, respectively. The results indicated that greater than 98% of the perchlorate on MR was reduced to chloride in 7 days. The biological treatment can be used to reduce perchlorate on spent MR for safely disposal of the material in non-hazardous waste landfills or for reuse.

5. Conclusions

This study demonstrates that quaternary amine modified reed, developed from the agricultural waste of giant reed, can be used as an effective adsorbent for the removal of perchlorate from aqueous solution. Perchlorate adsorption onto the modified reed occurred rapidly and reached equilibrium within 7 min. Kinetic results were well described by the pseudo second-order equation. Rapid boundary layer diffusion controlled the initial stage of adsorption at the monolayer while both boundary layer and intraparticle diffusion controlled adsorption at later stages. Optimum perchlorate

removal was achieved within the pH range (3.5–7.0). Zeta potential and Raman spectroscopy studies indicated that perchlorate removal by MR was achieved mainly by electrostatic interaction between perchlorate anions and quaternary amine functional groups in MR.

Acknowledgments

The authors thank the Center for Environmental systems (CES) and the Environment & Urban Development (EUD) for their support of this work.

References

[1] M.A. Greer, G. Goodman, R.C. Pleus, S.E. Greer, Health effects perchlorate contamination: the dose response for inhibition of thyroidal radioiodine uptake in humans, Environ. Health Perspect. 110 (2002) 927–937.
[2] P. Brandhuber, S. Clark, Perchlorate Occurrence Mapping, Prepared for the American Water Works Association, Washington, DC, 2005.
[3] J. Catts, Biological treatment of low level perchlorate contamination, in: Presented at the Perchlorate Stakeholders Forum, Henderson, Nevada, 1998.
[4] R. Sasse, Perchlorate treatment by ion exchange, in: Presented at the Perchlorate Stakeholders Forum, Henderson, Nevada, 1998.
[5] E.T. Urbansky, Perchlorate as an environnemental contaminant, Environ. Sci. Pollut. Res. 9 (2002) 187–192.
[6] D.R. Parker, A.L. Seyfferth, B.K. Reese, Perchlorate in groundwater: a synoptic survey of "pristine" sites in the coterminous United States, Environ. Sci. Technol. 42 (2008) 1465–1471.
[7] J.R. Clarkson, L. Yu, B.J. Locey, The toxicology of potential human health effects associated with perchlorate in drinking water, in: L. Hagström (Ed.), Perchlorate: A Scientific, Legal, and Economic Assessment, Lawyers & Judges Pub. Co., Arizona, 2006, pp. 87–89.
[8] M. Anbar, S. Guttmann, Z. Lewitus, Effect of monofluorosulphonate, difluorophosphate and fluoroborate ions on the iodine uptake of the thyroid gland, Nature 183 (1959) 1517–1518.
[9] A.B Kirk, Environmental perchlorate: why it matters, Anal. Chim. Acta 567 (2006) 4–12.
[10] S. Mukhi, L. Torres, R. Patino, Effects of larval–juvenile treatment with perchlorate and co-treatment with thyroxine on zebrafish sex ratios, Gen. Comp. Endocrinol. 150 (2007) 486–494.
[11] NRC (National Research Council), Health Implications of Perchlorate Ingestion, National Academy Press, Washington, DC, 2005, Available at: http://www.nap.edu/catalog.php?record_id=11202.
[12] K. Wirt, M. Laikhtman, J. Rohrer, P.E. Jackson, Low-level perchlorate analysis in drinking water and groundwater by ion chromatography, Am. Environ. Lab. 10 (1998) 1–5.
[13] G.M. Brown, B. Gu, The chemistry of perchlorate in the environment, in: B. Gu, J.D. Coates (Eds.), Perchlorate Environmental Occurrence Interactions and Treatment, Springer US, New York, 2006, pp. 17–47.
[14] P. Bunyan, A.V. Cunliffe, A. Davis, F.A. Kirby, The degradation and stabilisation of solid rocket propellants, Polym. Degrad. Stabil. 40 (1993) 239–250.
[15] C. Aziz, R. Borch, P. Nicholson, E. Cox, Alternative causes of wide-spread, low concentration perchlorate impacts to groundwater, in: B. Gu, J.D. Coates (Eds.), Perchlorate Environmental Occurrence Interactions and Treatment, Springer US, New York, 2006, pp. 71–91.
[16] W.A. Jackson, T. Anderson, G. Harvey, G. Orris, S. Rajagopalan, N. Kang, Occurrence and formation of non-anthropogenic perchlorate, in: B. Gu, J.D. Coates (Eds.), Perchlorate Environmental Occurrence Interactions and Treatment, Springer US, New York, 2006, pp. 49–69.
[17] E.T. Urbansky, Perchlorate chemistry: implications for analysis and remediation, Bioremed. J. 2 (1998) 81–95.
[18] A.R. Tripp, D.A. Clifford, The treatability of perchlorate in groundwater using ion exchange technology, in: E.T. Urbansky (Ed.), Perchlorate in the Environment, Springer US, New York, 2000, pp. 123–134.
[19] J.R. Batista, F.X. McGarvey, A.R. Vieira, The removal of perchlorate from waters using ion exchange resins, in: E.T. Urbansky (Ed.), Perchlorate in the Environment, Springer US, New York, 2000, pp. 135–146.
[20] Y. Cang, D.J. Roberts, D.A. Clifford, Development of cultures capable of reducing perchlorate and nitrate in high salt solutions, Water Res. 38 (2004) 3322–3330.
[21] B.E. Logan, J. Wu, R.F. Unz, Biological perchlorate reduction in high-salinity solutions, Water Res. 35 (2001) 3034–3038.
[22] A. Son, J. Lee, P.C. Chiu, B.J. Kim, D.K. Cha, Microbial reduction of perchlorate with zero-valent iron, Water Res. 40 (2006) 2027–2032.
[23] I.H. Yoon, X. Meng, C. Wang, K.W. Kim, S. Bang, E. Choe, L. Lippincott, Perchlorate adsorption and desorption on activated carbon and anion exchange resin, J. Hazard. Mater. 164 (2009) 87–94.
[24] C. Namasivayam, W.H. Hll, Quaternized biomass as an anion exchanger for the removal of nitrate and other anions from water, J. Chem. Technol. Biotechnol. 80 (2005) 164–168.
[25] Y. Wang, B.Y. Gao, W.W. Yue, Q.Y. Yue, Preparation and utilization of wheat straw anionic sorbent for the removal of nitrate from aqueous solution, J. Environ. Sci. 19 (2007) 1305–1310.
[26] U.S. Orlando, A.U. Baes, W. Nishijima, M. Okada, A new procedure to produce lignocellulosic anion exchangers from agricultural waste materials, Bioresour. Technol. 83 (2002) 195–198.
[27] B.Y. Gao, X. Xu, Y. Wang, Q.Y. Yue, X.M. Xu, Preparation and characteristics of quaternary amino anion exchanger from wheat residue, J. Hazard. Mater. 165 (2009) 461–468.
[28] R.E. Perdue, Arundo donax: source of reeds and industrial cellulose, Econ. Bot. 12 (1958) 368–404.
[29] A.A. Shatalov, H. Pereira, Influence of stem morphology on pulp and paper properties of Arundo donax L. reed, Ind. Crop Prod. 15 (2002) 77–83.
[30] T. Vernersson, P.R. Bonelli, E.G. Cerrella, A.L. Cukierman, Arundo donax cane as a precursor for activated carbons preparation by phosphoric acid activation, Bioresour. Technol. 83 (2002) 95–104.
[31] P.A. Anthony, The macrofungi and decay of roofs thatched with water reed, *Phragmites Australis*, Mycol. Res. 103 (1999) 1346–1352.
[32] Q.Y. Yue, W.Y. Wang, B.Y. Gao, X. Xu, J. Zhang, Q. Li, Phosphate removal from aqueous solution by adsorption on modified giant reed, Water Environ. Res. 82 (2010) 374–381.
[33] U.S. Orlando, T. Okuda, A.U. Baes, W. Nishijima, M. Okada, Chemical properties of anion-exchangers prepared from waste natural materials, React. Funct. Polym. 55 (2003) 311–318.
[34] W.Y. Wang, Q.Y. Yue, X. Xu, B.Y. Gao, J. Zhang, Q. Li, J.T. Xu, Optimized conditions in preparation of giant reed quaternary amino anion exchanger for phosphate removal, Chem. Eng. J. 157 (2010) 161–167.
[35] Q.Y. Yue, W.Y. Wang, B.Y. Gao, X. Xu, J. Zhang, Q. Li, Sorption of phosphate onto giant reed based adsorbent: FTIR, Raman spectrum analysis and dynamic sorption/desorption properties in filter bed, Bioresour. Technol. (2010), doi:10.1016/j.bioretech.2010.10.130.
[36] T.H. Kim, M. Jang, J.A. Park, Bifunctionalized mesoporous molecular sieve for perchlorate removal, Microporous Mesoporous Mater. 108 (2008) 22–28.
[37] R.J. Hunter, Zeta Potential in Colloid Science: Principles and Applications (1981), Academic Press, New York, 1981.
[38] Y. Wang, B.Y. Gao, W.W. Yue, Q.Y. Yue, Adsorption kinetics of nitrate from aqueous solutions onto modified wheat residue, Colloids Surf., A 308 (2007) 1–5.
[39] Y.S. Ho, G. McKay, The kinetics of sorption of divalent metal ions onto sphagnum moss peat, Water Res. 34 (2000) 735–742.
[40] C.H. Bolster, G.M. Hornberger, On the use of linearized Langmuir equations, Soil Sci. Soc. Am. J. 71 (2007) 1796–1806.
[41] E.I. Unuabonah, K.O. Adebowale, F.A. Dawodu, Equilibrium, kinetic and sorber design studies on the adsorption of Aniline blue dye by sodium tetraborate-modified Kaolinite clay adsorbent, J. Hazard. Mater. 157 (2008) 397–409.
[42] Z. Aksu, I.A. Isoglu, Use of agricultural waste sugar beet pulp for the removal of Gemazol turquoise blue-G reactive dye from aqueous solution, J. Hazard. Mater. 137 (2006) 418–430.
[43] M. Ramakrishnan, N. Sulochana, Utilization of waste biomass for the removal of basic dye from water, World Appl. Sci. J. 5 (2009) 114–121.
[44] B. Koumanova, P. Peeva, S.J. Allen, Variation of intraparticle diffusion parameter during adsorption of chlorophenol onto activated carbon made from apricot stones, J. Chem. Technol. Biotechnol. 78 (2003) 582–587.
[45] W.J. Weber, J.C. Morris, Kinetics of adsorption on carbon from solution, J. Sanit. Eng. Div. Am. Soc. Civ. Eng. 89 (1963) 31–60.
[46] M. Dutta, R. Baruah, N.N. Dutta, A.C. Ghosh, The adsorption of certain semi-synthetic cephalosporins on activated carbon, Colloids Surf., A 127 (1997) 25–37.
[47] G. McKay, M.S. Otterburn, A.G. Sweeney, The removal of colour from effluent using various adsorbents—III. Silica: rate processes, Water Res. 14 (1980) 15–20.
[48] B.H. Hameed, M.I. El-Khaiary, Kinetics and equilibrium studies of malachite green adsorption on rice straw-derived char, J. Hazard. Mater. 153 (2008) 701–708.
[49] I. Langmuir, The adsorption of gases on plane surfaces of glass, mica and platinum, J. Am. Chem. Soc. 40 (1918) 1361–1403.
[50] N.Z. Misak, Adsorption isotherms in ion exchange reactions. Further treatments and remarks on the application of the Langmuir isotherm, Colloids Surf., A 97 (1995) 129–140.
[51] R. Mahmudov, C.P. Huang, Perchlorate removal by activated carbon adsorption, Sep. Purif. Technol. (2009) 329–337.
[52] R. Apak, Adsorption of heavy metal ions on soil surfaces and similar substances: theoretical aspects, in: P. Somasundaran (Ed.), Encyclopedia of Surface and Colloid Science: Second Edition, Taylor & Francis, New York, 2006, pp. 494–509.
[53] P. Srivastava, B. Singh, M. Angove, Competitive adsorption behavior of heavy metals on kaolinite, J. Colloid Interface Sci. 290 (2005) 28–38.
[54] H. Freundlich, Colloid and Capillary Chemistry, Methuen & Co., London, 1926.
[55] G. Sposito, Derivation of the Freundlich equation for ion exchange reactions in soils, Soil Sci. Soc. Am. J. 44 (1980) 652–654.
[56] K.R. Hall, L.C. Eagleton, A. Acrivos, T. Vermeulen, Pore- and solid-diffusion kinetics in fixed-bed adsorption under constant-pattern conditions, Ind. Eng. Chem. Fundam. 5 (1966) 212–223.
[57] B.P. Binks, Particles as surfactants—similarities and differences, Curr. Opin. Colloid Interface Sci. 7 (2002) 21–41.
[58] Y. Ikada, E. Uchida, Zeta-potential of polymer surfaces, in: P. Somasundaran (Ed.), Encyclopedia of Surface and Colloid Science: Second Edition, Taylor & Francis, New York, 2006, pp. 6665–6675.
[59] R.A. Silva, G.G. Silva, M.A. Pimenta, Micro-Raman study of polydioxolane/LiClO and NaClO electrolytes, Appl. Phys. Lett. 67 (1995) 3352–3354.

[60] S. Schantz, L.M. Torell, J.R. Stevens, Ion pairing effects in poly (propylene glycol)–salt complexes as a function of molecular weight and temperature: a Raman scattering study using $NaCF_3SO_3$ and $LiClO_4$, J. Chem. Phys. 94 (1991) 6862–6867.
[61] N.D. Cvjeticanin, S. Sasic, Raman spectroscopic study of lithium and sodium perchlorate association in propylene carbonate–water mixed solvents, J. Raman Spectrosc. 31 (2000) 871–876.
[62] T.G. Levitskaia, S.I. Sinkov, S.A. Bryan, In situ perchlorate determination on Purolite A850 ion exchange resin, Vib. Spectrosc. 44 (2007) 316–323.
[63] B. Gu, J. Tio, W. Wang, Y.K. Ku, S. Dai, Raman spectroscopic detection for perchlorate at low concentrations, Appl. Spectrosc. 58 (2004) 741–744.
[64] P.A. Mosier-Boss, S.H. Lieberman, Detection of anions by normal Raman spectroscopy and surface-enhanced Raman spectroscopy of cationic-coated substrates, Appl. Spectrosc. 54 (2003) 1129–1137.
[65] A.G. Miller, J.A. Franz, J.W. Macklin, Chlorine-35 nuclear magnetic resonance study of aqueous sodium perchlorate association, J. Phys. Chem. 89 (1985) 1190–1193.
[66] P.A. Brooksby, W.R. Fawcett, Infrared (attenuated total reflection) study of propylene carbonate solutions containing lithium and sodium perchlorate, Spectrochim. Acta, Part A 64 (2006) 372–382.
[67] C. Wang, L. Lippincott, X.G. Meng, Kinetics of biological perchlorate reduction and pH effect, J. Hazard. Mater. 153 (2008) 663–669.